Supporting Information

Biodegradable MoO_x nanoparticles with efficient near-infrared photothermal and photodynamic synergetic cancer therapy at the second biological window

Wenyan Yin[a], Tao Bao[a], Xiao Zhang[a], Qin Gao[a], Jie Yu[a], Xinghua Dong[a], Liang Yan[a], Zhanjun Gu[a,*] and Yuliang Zhao[a,b]

[a]Key Laboratory for Biomedical Effects of Nanomaterials and Nanosafety, Institute of High Energy Physics, Chinese Academy of Sciences, Beijing 100049, China

[b]National Center for Nanosciences and Technology of China, Beijing 100190, China,

Corresponding Authors: zjgu@ihep.ac.cn

Measurement of Photothermal Performance

The conversion efficiency (η) is an important character for photothermal materials. To measure the photothermal conversion efficiency (η), the PEG-MoO_x NPs water solutions with the test concentration were exposed to NIR 808 nm and 1064 nm CW laser, respectively (1.0 W/cm^2) for 10 min, and then the laser was shut off. The heating and cooling temperature trends of the samples were recorded by FLIR thermal camera (Fig. S4). And, the photothermal conversion efficiency was calculated according to the eq. 1: [1, 2]

$$\eta = \frac{hS\left(T_{\max} - T_{surr}\right) - Q_0}{I\left(1 - 10^{-A}\right)} \quad (1)$$

Where h is the heat transfer coefficient, S is the surface area of the container, T_{max} is the steady state maximum temperature, T_{surr} is the ambient temperature of the surroundings, Q_0 is the baseline energy input by the solvent and the sample container without PEG-MoO_x NPs, I is the laser power, and A is the absorbance of PEG-MoO_x NPs solution at 808 nm or 1064 nm. The value of hS is calculated by eq. 2:

$$\tau_s = \frac{m_d C_d}{hS} \quad (2)$$

Where τ_s is the characteristic thermal time constant (Fig. S2d and S3d), the mass of the m_d and C_d are the mass and heat capacity of water, respectively. The heat energy (Q_0) of the sample container and solvent without PEG-MoO_x NPs were measured independently using the eq. 3:

$$Q_0 = hS(T_{\max} - T_{surr}) \quad (3)$$

Finally, the 808 nm and 1064 nm laser induced photothermal conversion efficiency (η) of the PEG-MoO_x NPs were calculated as ~27.3% and 37.4%, respectively.

References:

[1] Liu J, Zheng X, Yan L, Zhou L, Tian G, Yin W, et al. Bismuth Sulfide Nanorods as a Precision Nanomedicine for in Vivo Multimodal Imaging-Guided Photothermal Therapy of Tumor. ACS Nano. 2015, 9, 696-707.

[2] Tian Q, Hu J, Zhu Y, Zou R, Chen Z, Yang S, et al. Sub-10 nm Fe_3O_4@$Cu_{2-x}S$ Core–Shell Nanoparticles for Dual-Modal Imaging and Photothermal Therapy. J. Am. Chem. Soc. 2013, 135, 8571-8577.

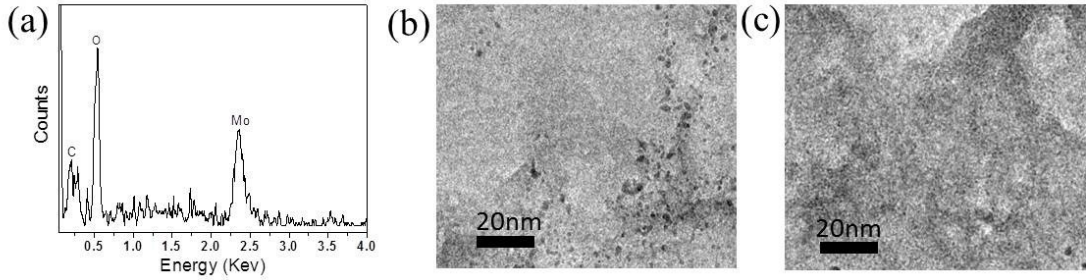

Figure S1. (a) EDX spectrum of the PEG-MoO_x NPs. TEM images of degradation process of PEG-MoO_x NPs incubated with PBS buffer (pH=7.4) with prolonged incubation time (b) 48 h and (c) 72 h.

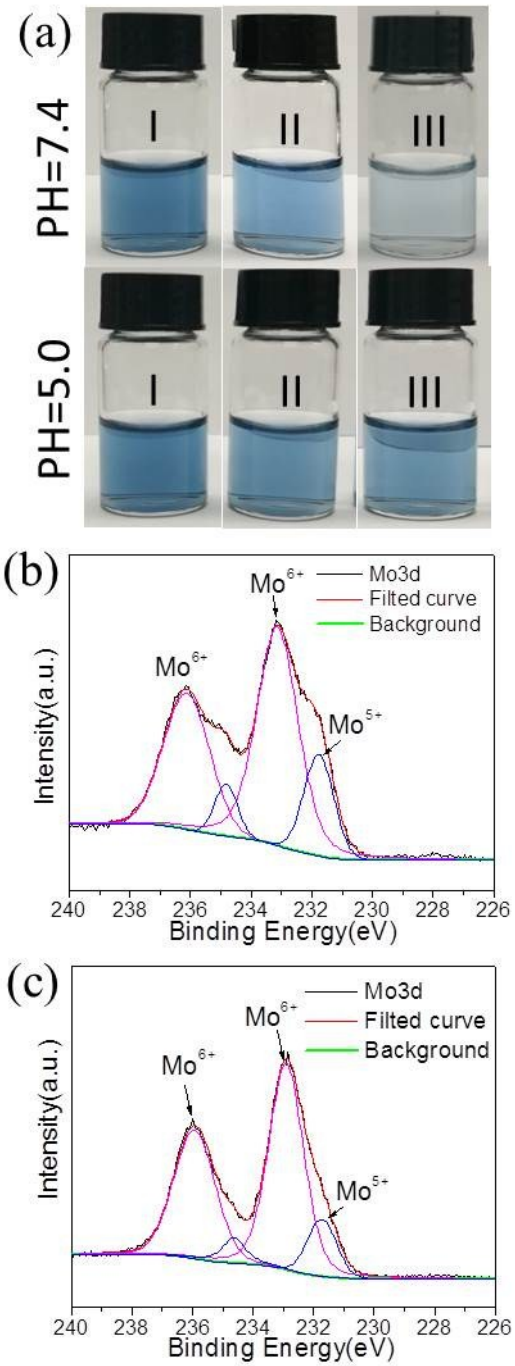

Figure S2. (a) The photos of color change during the degradation process of PEG-MoO_x NPs with concentrations of 200 μg/mL in PBS (pH=7.4) at fixed time intervals 0 h, 48 h, and 72 h. Mo3d peaks in XPS spectra of PEG-MoO_x after being incubated in PBS at pH 7.4 for (b) 48 h and (c) 72 h during the degradation process.

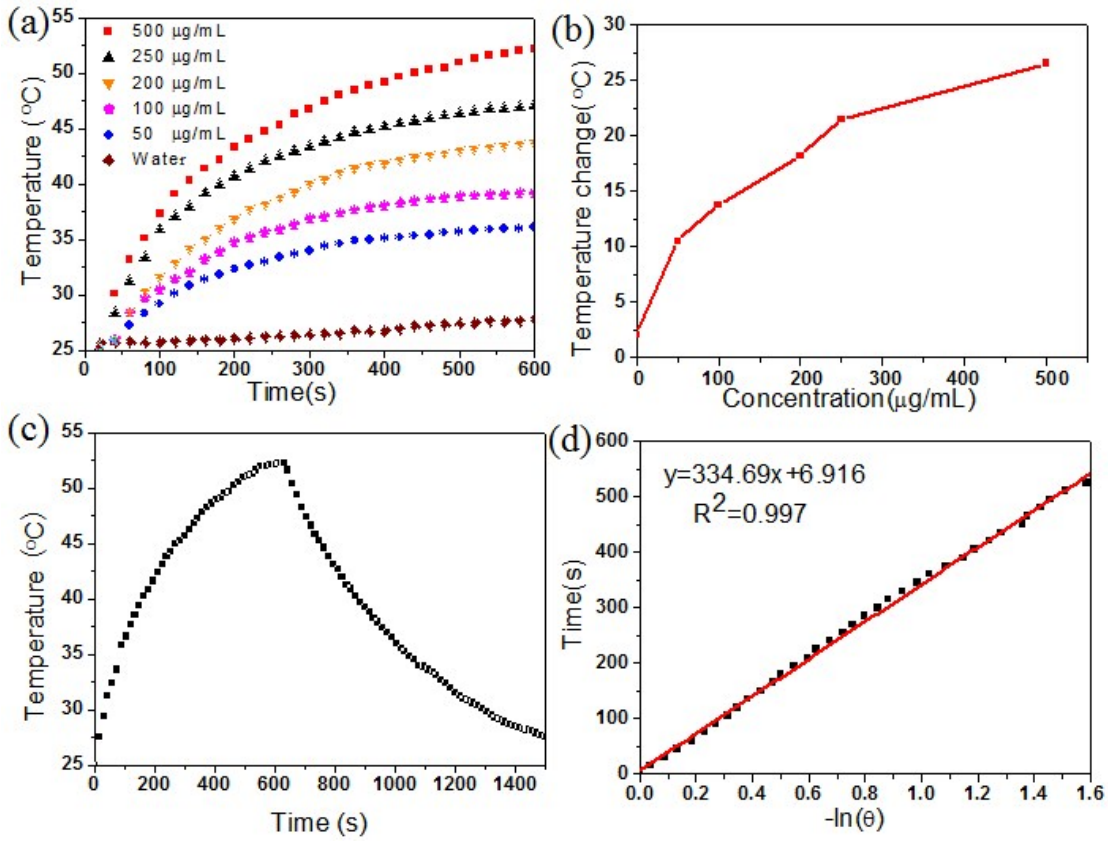

Figure S3. (a) Photothermal heating curves of PEG-MoO_x NPs aqueous dispersion with different concentrations under 808 nm laser irradiation at the power density of 1.0 W/cm^2. (b) Temperature change of PEG-MoO_x NPs aqueous dispersion at different concentrations under 808 nm laser irradiation for 600 s. (c) Photothermal response of PEG-MoO_x NPs dispersion (200 μg/mL) under 808 nm NIR laser irradiation, and then the laser was shut off. (d) Plot of cooling time *versus* negative natural logarithm of the temperature driving force which is obtained from the cooling stage. Time constant for heat transfer from the system is determined to be τs = 334.69 s.

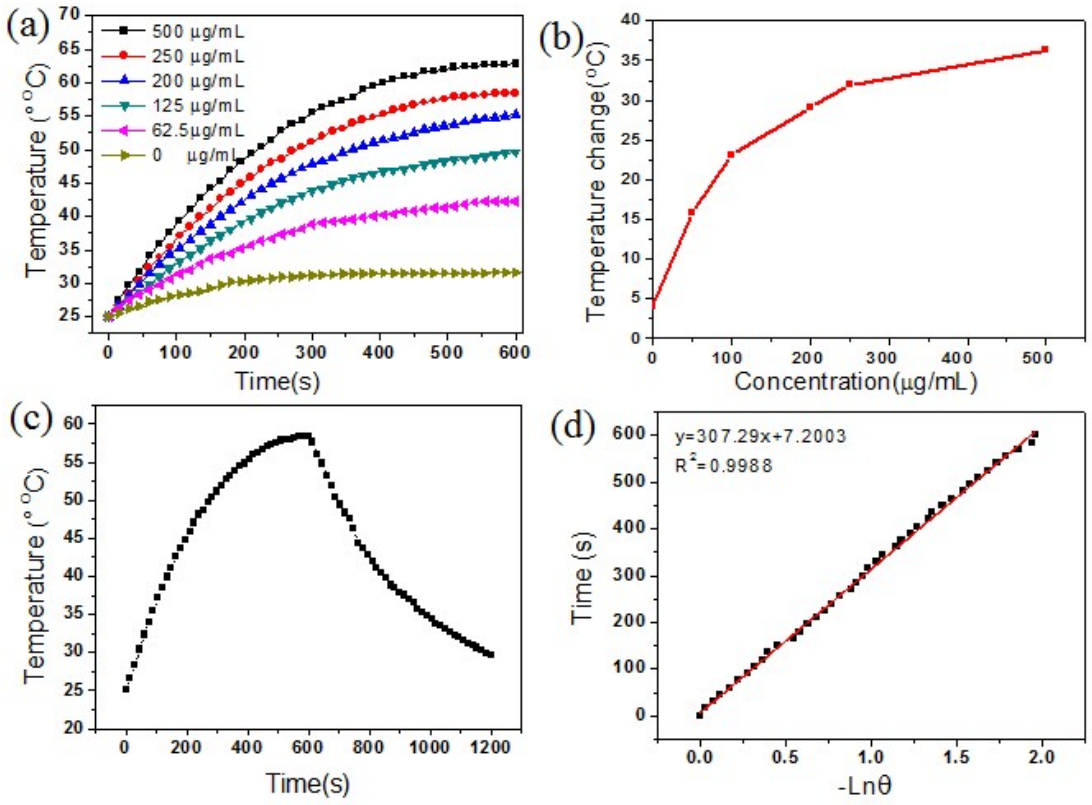

Figure S4. (a) The photothermal heating curves of PEG-MoO_x NPs aqueous dispersion with different concentrations under exposure to 1064 nm laser at the power density of 1.0 W/cm^2. (b) Temperature change of PEG-MoO_x NPs aqueous dispersion at different concentrations under 1064 nm laser irradiation for 600 s. (c) Photothermal response of PEG-MoO_x NPs dispersion (250 μg/mL) under 1064 nm laser irradiation, and then the laser was shut off. (d) Plot of cooling time versus negative natural logarithm of the temperature driving force which is obtained from the cooling stage. Time constant for heat transfer from the system is determined to be τs = 307.29s.

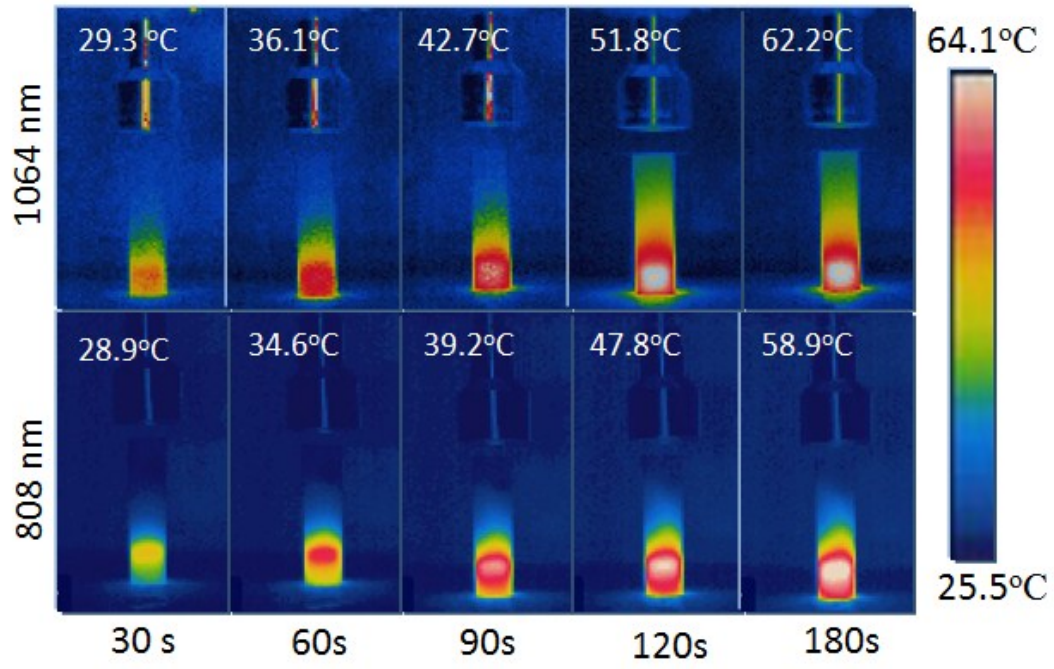

Figure S5. Infrared thermal images of PEG-MoO_x NPs aqueous dispersion with the concentration of 500 μg mL^{-1} under 808 nm and 1064 nm laser irradiation at the power density of 1.0 W/cm^2. The joint spider stand for the irradiated spot of the NIR laser.

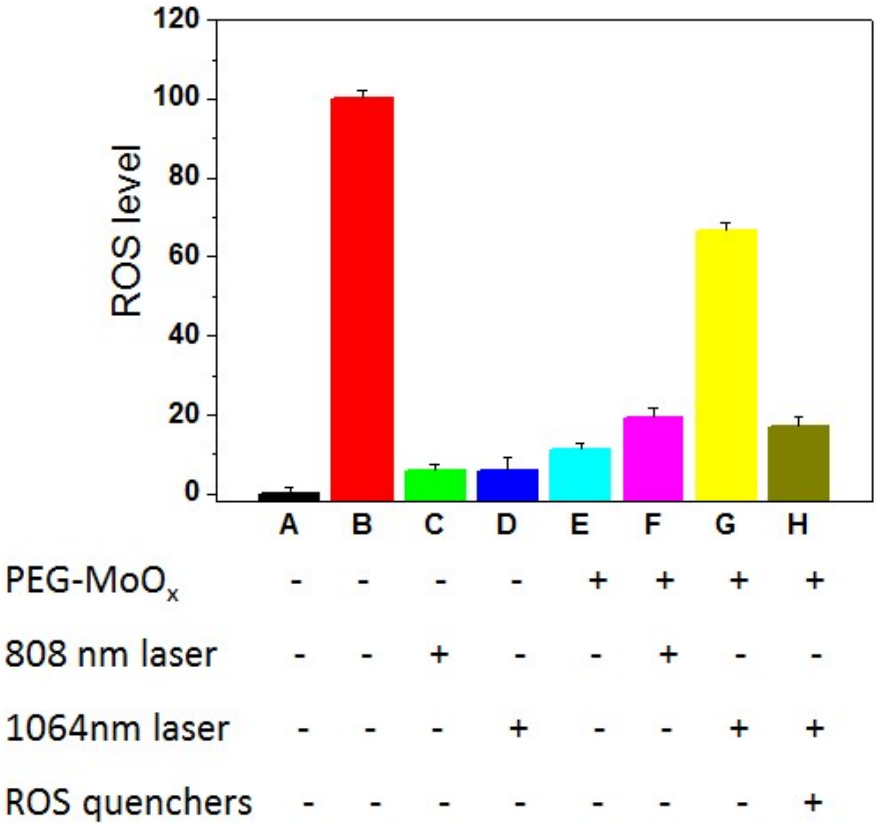

Figure S6. Quantitative comparison of ROS generation in Fig. 5. Data are shown as mean (the standard error from more than 20 independent cells).

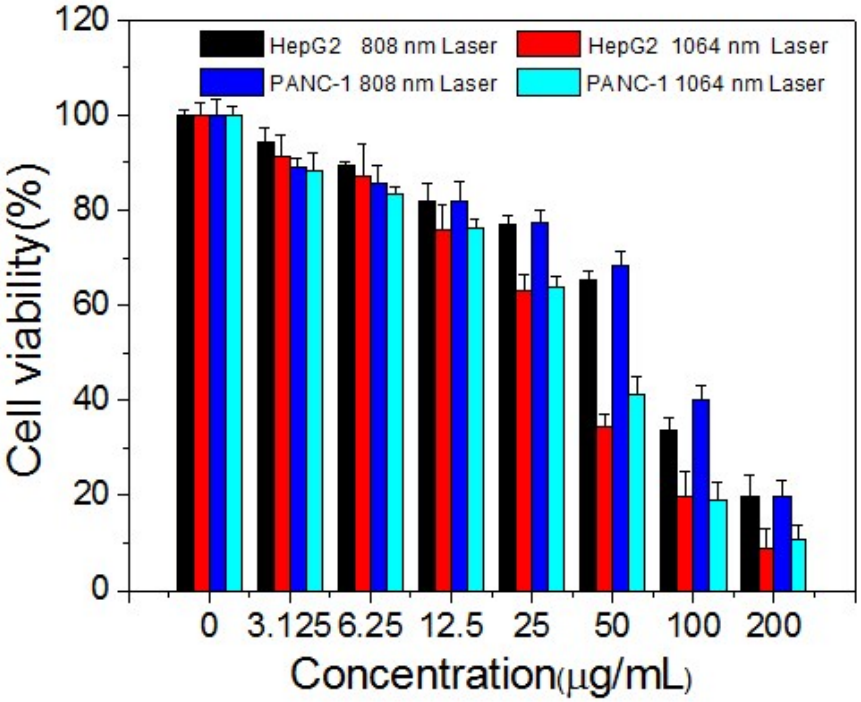

Figure S7. Cell viabilities of PANC-1 and HepG2 cells treated with PEG-MoO_x NPs under 808 nm (power density: 1.2 W/cm^2) and 1064 nm (power density: 1.0 W/cm^2) laser irradiation.

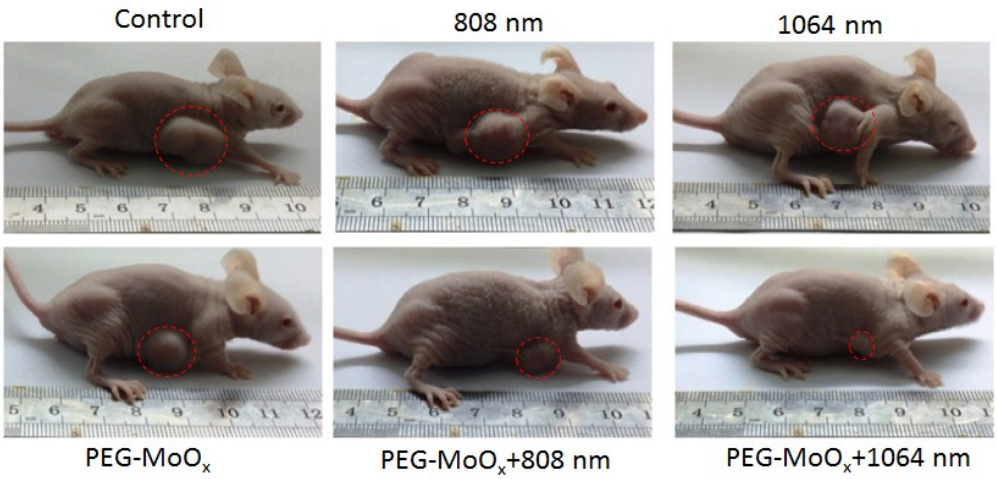

Figure S8. Typical photographs of the tumor-bearing mice at different treatment groups. The red circles were marked as tumor sites.